

UCLA

UCLA Previously Published Works

Title

Environmental drivers of spatial variation in tropical forest canopy height: Insights from NASA's GEDI spaceborne LiDAR

Permalink

<https://escholarship.org/uc/item/69q6g5js>

Journal

Proceedings of the National Academy of Sciences of the United States of America, 122(10)

ISSN

0027-8424

Authors

Liu, Shaoqing
Csillik, Ovidiu
Ordway, Elsa M
[et al.](#)

Publication Date

2025-03-11

DOI

10.1073/pnas.2401755122

Copyright Information

This work is made available under the terms of a Creative Commons Attribution License, available at <https://creativecommons.org/licenses/by/4.0/>

Peer reviewed



Environmental drivers of spatial variation in tropical forest canopy height: Insights from NASA's GEDI spaceborne LiDAR

Shaoqing Liu^{a,1}, Ovidiu Csillik^{b,c}, Elsa M. Ordway^d, Li-Ling Chang^{a,e}, Marcos Longo^f, Michael Keller^{b,g}, and Paul R. Moorcroft^h

Edited by Christopher Field, Stanford University, Stanford, CA; received February 3, 2024; accepted January 9, 2025

Forest canopy height is a fundamental ecosystem property—influencing patterns of forest carbon storage and forest ecosystem responses to climate variability and change. Previous studies have analyzed environmental drivers influencing spatial variation in canopy height at landscape-to-regional scales; however, far less is known about the environmental determinants underlying regional and global scale variation in forest canopy height. Using the canopy height metrics products from Global Ecosystem Dynamics Investigation (GEDI), a space-borne Light Detection and Ranging (LiDAR) instrument specifically designed to characterize forest structure, we analyze the environmental correlates of spatial variation of global tropical forest canopy height. Our study demonstrates that climate, topography, and soil properties account for 75% of the variation in tropical forest canopy height. Elevation, dry season length, and solar radiation are the most important drivers in determining canopy height both locally and regionally. These results emphasize the vulnerability of tropical forest structure to ongoing changes in the earth's climate and provide a valuable empirical baseline for tropical forest management.

tropical forest | GEDI | canopy height

Canopy height is a key attribute of forest ecosystems influencing their above-ground biomass (1, 2), forest resilience to drought (3), and tree mortality (4, 5). Canopy height also correlates with plant and animal diversity (6, 7). Accordingly, canopy height information has been used as an important source of measurements informing initiatives for carbon accounting, climate change mitigation via natural carbon sinks (2, 8, 9), constraining and improving terrestrial ecosystem and biosphere model predictions (10, 11), and guiding conservation priorities (12, 13).

Ground-based forest inventories have been traditionally used to measure and quantify the structural attributes of forest canopies, such as canopy height, stem density, and stem basal area. Such inventories collect detailed tree-level information from a series of plots across a given landscape; however, the plots are typically small (in some cases 0.1 to 0.5 km², but frequently less than 0.01 km²), and widely spaced across the landscape. Consequently, plot networks may often be unrepresentative of the wider landscape, particularly in tropical regions. For example, a network of 413 field inventory plots, covering less than 0.01% of the Amazon Basin, has been widely used to represent Amazonian forests. The high costs of field data collection also poses significant challenges leading efforts to prioritize representativeness over coverage (14).

Remote sensing is revolutionizing our understanding of forest ecosystems by providing spatially comprehensive and consistent measurements of forest biophysical attributes. LiDAR measurements can provide detailed, three-dimensional information of forest canopy structure. Other active remote sensing instruments can provide complementary information about forest canopies: Synthetic aperture radar (SAR) can provide information about their surface roughness, moisture content, and above-ground biomass, and optical remote sensing measurements can provide information about land-cover and forest canopy characteristics, including measures of canopy greenness, moisture content, and leaf properties (15, 16). Airborne and unmanned aerial vehicle small footprint and waveform LiDAR are also increasingly being used to measure forest canopy height across landscapes at high spatial resolution, especially in tropical ecosystems where the regional-scale forest inventories are less available (17–21).

Local and regional scale studies have shown that forest canopy height exhibits strong spatial variation that is linked to a number of environmental drivers, including precipitation, temperature, solar radiation, soil texture, soil moisture content, and soil nutrient, and natural and human disturbance history, and biogeographical history (22, 23). At global scales, an analysis of tree heights using 7,042 tree height records from 5,784 tree species distributed across 222 locations (24), found that precipitation in the wettest month

Significance

In this study, measurements from NASA's Global Ecosystem Dynamics Investigation spaceborne LiDAR mission are used to understanding global-scale patterns of tropical forest canopy height. The study shows that elevation, dry season length, and solar radiation are key drivers in determining tropical forest canopy height both locally and regionally. These findings are relevant to understanding tropical forest responses to climate variability and change and for forest carbon management and conservation strategies.

Author affiliations: ^aDepartment of Organismic and Evolutionary Biology, Harvard University, Cambridge, MA 02138; ^bJet Propulsion Laboratory, California Institute of Technology, Pasadena, CA 91109; ^cEnvironment and Sustainability Studies Program, Wake Forest University, Winston-Salem, NC 27109; ^dDepartment of Ecology and Evolutionary Biology, University of California, Los Angeles, CA 90095; ^eDepartment of Geography, Florida State University, Tallahassee, FL 32306; ^fClimate and Ecosystem Sciences Division, Lawrence Berkeley National Laboratory, Berkeley, CA 94720; and ^gInternational Institute of Tropical Forestry, United States Department of Agriculture Forest Service, Rio Piedras 00926, Puerto Rico

Author contributions: S.L. and P.R.M. designed research; S.L. and P.R.M. performed research; S.L., O.C., E.M.O., L.C., M.L., M.K., and P.R.M. contributed new reagents/analytic tools; S.L., O.C., E.M.O., L.C., M.L., M.K., and P.R.M. analyzed data; and S.L., O.C., E.M.O., L.C., M.L., M.K., and P.R.M. wrote the paper.

The authors declare no competing interest.

This article is a PNAS Direct Submission.

Copyright © 2025 the Author(s). Published by PNAS. This article is distributed under [Creative Commons Attribution-NonCommercial-NoDerivatives License 4.0 \(CC BY-NC-ND\)](https://creativecommons.org/licenses/by-nc-nd/4.0/).

Although PNAS asks authors to adhere to United Nations naming conventions for maps (<https://www.un.org/geospatial/mapsgeo>), our policy is to publish maps as provided by the authors.

¹To whom correspondence may be addressed. Email: shaoqingliu@fas.harvard.edu.

This article contains supporting information online at <https://www.pnas.org/lookup/suppl/doi:10.1073/pnas.2401755122/-/DCSupplemental>.

Published March 3, 2025.

of the year was the single strongest predictor of plant height, but other explanatory drivers, such as minimum temperature in the coldest month and elevation explained surprisingly little of the observed variation in plant height. In addition, measurements from the Geoscience Laser Altimeter System (GLAS) waveform lidar aboard the Ice, Cloud, and land Elevation Satellite (ICESat) have been used in conjunction with spatial variation in environmental drivers to map global forest canopy height (25), and several studies have sought to understand the global-scale patterns of forest canopy height using height estimates derived from ICESat observations (26, 27). However, due to the relatively low sampling density of ICESat measurements, particularly in tropical forests (28), the canopy height estimates used in these studies were not direct measurements, but rather outputs from a statistical model that spatially interpolated ICESat LiDAR retrievals using climatic drivers, rather than direct LiDAR observations.

The Global Ecosystem Dynamics Investigation (GEDI) on the International Space Station is the first spaceborne LiDAR specifically designed to characterize the three-dimensional forest structure at large scales (51.6°S to 51.6°N) (29). The GEDI mission is a full waveform LiDAR instrument operating at 1,064 nm, which samples forest structure with footprints of 25 m in diameter, every 60 m along its ascending and descending orbital paths (29). In comparison, the GLAS-ICESat produces 1,064 nm pulses estimates canopy height within 30 to 70 m diameter footprint approximately every 170 m (30). More recently, the IceSat-2 ATLAS mission operates at 532 nm, offering improved spatial resolution with 14 m diameter footprints and along-track spacing of 0.7 m. Various mapping efforts have successfully combined GEDI and/or IceSat-2 sampling with optical imagery to enhance forest structure assessments (31–33). For example, Potapov et al. (31) integrates GEDI lidar and Landsat data to create a global 30 m resolution forest canopy height map for 2019. Validated against GEDI and airborne lidar data, the map enables monitoring of forest height, aiding carbon emission estimates and forest management efforts. The GEDI mission represents a significant advancement over these previous LiDAR missions by providing higher resolution and more comprehensive data and therefore provides a unique opportunity to understand the spatial distribution of canopy height across the tropical forest biomes.

In this study, we analyze the level 2A GEDI geolocated elevation and height metrics product (version 2) to understand how environmental drivers shape the spatial distribution of tropical forest canopy height. Specifically, we focus on tropical moist forest ecosystems because of their critical role in the global carbon cycle, accounting for one-third of terrestrial primary production and 25% of stored terrestrial carbon (34). We performed analyses relating climatic drivers, topography, and soil properties to the spatial variation in forest canopy height as measured by GEDI Level 2A height measurements. The specific goals of the analyses were to: 1) identify which key environmental drivers control forest canopy height across the earth's tropical forest regions, and 2) determine how the key drivers affecting local forest canopy height vary spatially across the tropics.

Prior to the analysis, multiple data sources were used to minimize the effects of human disturbance on study's findings. Starting from the map of intact tropical humid forests in 2001 (35), a dataset of forest extent and height changes was used to exclude areas that have experienced forest loss or significant disturbances between 2000 and 2020 (36) (see the *Methods Summary* section). Additionally, GEDI shots classified as nonforest based on the MODIS-derived GEDI L2A supplementary data fields were excluded. Further details on the methods employed can be found in the *Methods Summary* section.

Results

Analysis of the spatial distribution of GEDI canopy heights across the tropics shows that the tallest tropical forest canopies are primarily located in the Eastern Amazon Basin, Gabon, and Borneo (Fig. 1A). Although the Amazon, Africa, and Southeast Asian tropical regions have relatively similar average canopy height (means of 27.0 m, 29.6 m, and 33.0 m for Amazon, African, and Southeast Asian tropical forests respectively), Southeast Asia has a higher proportion of tall tropical trees, as indicated by the more right-skewed histogram forest canopy heights (Fig. 1B). For example, the percentage of forest canopy heights greater than 40 m in Southeast Asia is 15.6.8%, compared to 8.5% in Africa and 4.2% in the Amazon.

A correlation analysis was first conducted to investigate the simple univariate relationships between canopy height and a series of environmental drivers across all tropical regions. Canopy height exhibits notable significant positive correlations with elevation and cloudiness, and negative correlations with wind speed, dry season length (DSL), and soil sand fraction (Fig. 1C). In contrast, canopy height exhibits weak correlations with precipitation, temperature seasonality, solar radiation, lightning frequency, and soil organic matter content (Fig. 1C).

Less than 0.05% of the canopy height measurements in the GEDI shots analyzed here are extremely tall [greater than 70m (19)]; however, our analysis shows that extremely tall trees are strongly clustered toward the center of a Principal Components ordination of the environmental conditions associated with the GEDI canopy height measurements (*SI Appendix, Fig. S6*), indicating that their occurrence peaks in areas with combination of moderate environmental conditions (e.g., precipitation, dry season length, and temperature seasonality) rather than in locations with particularly high or low values of specific environmental drivers. However, the center of the very tall tree distribution is noticeably negatively offset with respect to wind, lightning, and incoming solar radiation vectors, indicating that extremely tall trees tend to be associated with low values of these environmental drivers.

To further explore the combined influences and importance of the different environmental drivers in determining spatial variation in canopy height across the tropics, we employed a random-forest (RF) machine learning algorithm (37). In contrast to correlation, RF can capture complex relationships that are often missed in simple pairwise analysis, making it a more powerful tool for prediction. In terms of overall goodness-of-fit, the RF model captures 75% of the observed variation in tropical forest canopy height ($R^2 = 0.75$, Fig. 2A). More detailed examination of the model's goodness-of-fit shows that the model captures the observed pattern of variation in tree heights below a height of 45 m well; however, it tends to underestimate canopy height above this value (Fig. 2A), in large part due to the relatively smaller number (~810,000, accounting for only 1.44% of the filtered GEDI shots, see *Method Summary*) of tall forest canopies within the GEDI dataset (Fig. 1B). The three most important explanatory environmental drivers in the random forest model at the continental scale are elevation, dry season length, and solar radiation (feature importance values of 0.165, 0.152, and 0.128 respectively, see Fig. 2B).

While the RF model effectively ranks feature importance across the entire study area, it offers limited insights into how these features influence predictions at local scale. We therefore employed a Local Interpretable Model-Agnostic Explanations (LIME) framework to determine the most important environmental drivers in governing canopy height in each grid cell across the three continents (*Methods Summary*).

As seen in Fig. 3A, the most important predictors of canopy height vary across different regions. In South America, DSL is the

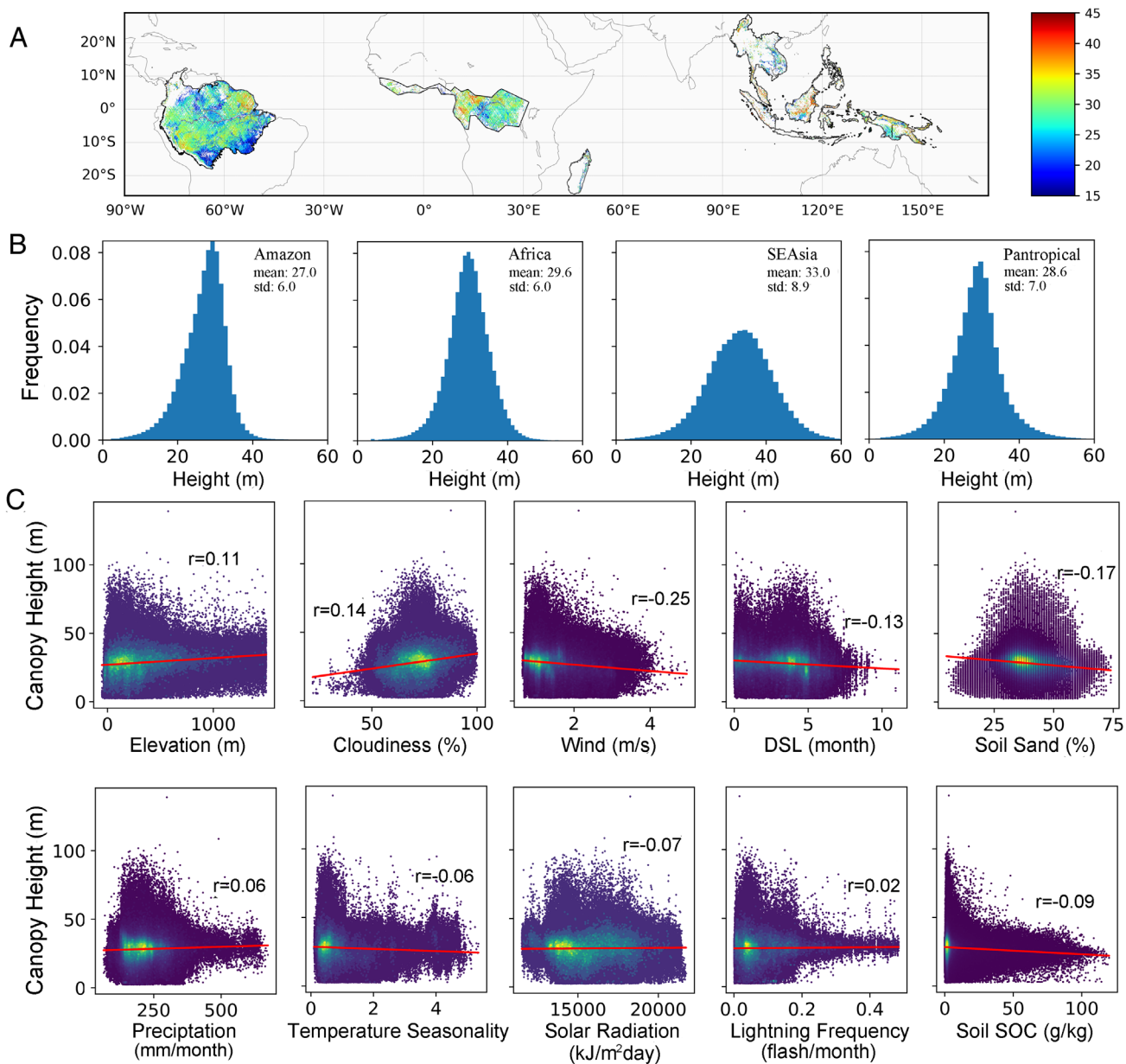


Fig. 1. (A) Distribution of canopy height derived from quality-filtered GEDI L2A shots. (B) Histogram of canopy heights for the Amazon, Africa, Southeast Asia and Pantropical regions. (C) The linear relationship between canopy height and the environmental drivers across the pantropical region.

dominant predictor of canopy height in the western and southern Amazon while elevation is the dominant predictor in the Amazon floodplain. In Africa, elevation is the dominant predictor of canopy height across much of the continent; however, in parts of Madagascar and west Africa, DSL and other climate drivers are more important. Finally, in Southeast Asia, elevation is the dominant predictor for most regions except for parts of Northern Myanmar, Laos, Borneo and Papua New Guinea where DSL dominates (Fig. 3A). Solar radiation is rarely the first (most important) predictor identified by the RF-based LIME analysis (Fig. 3A); however, it is the third-most frequent second predictor (Fig. 3B), and it is the most frequent third predictor (Fig. 3C). Further details on the environmental drivers by the RF-based LIME analysis as key predictors of canopy height can be found in *SI Appendix, Table S1*.

We conducted a marginal analysis on the fitted RF model to further explore how the different environmental drivers may affect spatial variation of canopy height across the tropics. While the feature importance of the RF model provides a broad overview of the relative importance of the different environmental drivers

influencing canopy height, the marginal analysis enables us to explore and visualize how variation in a particular driver—such as precipitation or temperature—affects forest canopy height. Fig. 4 A–F shows marginal plots of the six most important explanatory drivers from Fig. 2B. Between elevations of 0 m to 200 m, average canopy height increases from 24 m to 32 m and then declines slightly above 600 m (Fig. 4A). In contrast, DSL exhibits a nonlinear, threshold-type relationship, with minor changes in average canopy height below 4 mo DSL followed by a marked, 8 m decline in average canopy height when DSL exceeds this value (Fig. 4B). The effect of solar radiation on average canopy height is also nonlinear relationship with minimal effect on canopy height when the solar radiation is below 14,000 kJ m⁻² d⁻¹, followed by a decline of 4 m when radiation increases above 15,000 kJ m⁻² d⁻¹ and then an increase of 3 m when radiation is above 17,000 kJ m⁻² d⁻¹ (Fig. 4C). The effects of temperature seasonality on canopy height are negative, with canopy height declining an average of 7 m when the temperature seasonality increases from 0 °C to above 2 °C (Fig. 4D). Wind speed and cloudiness are also significant

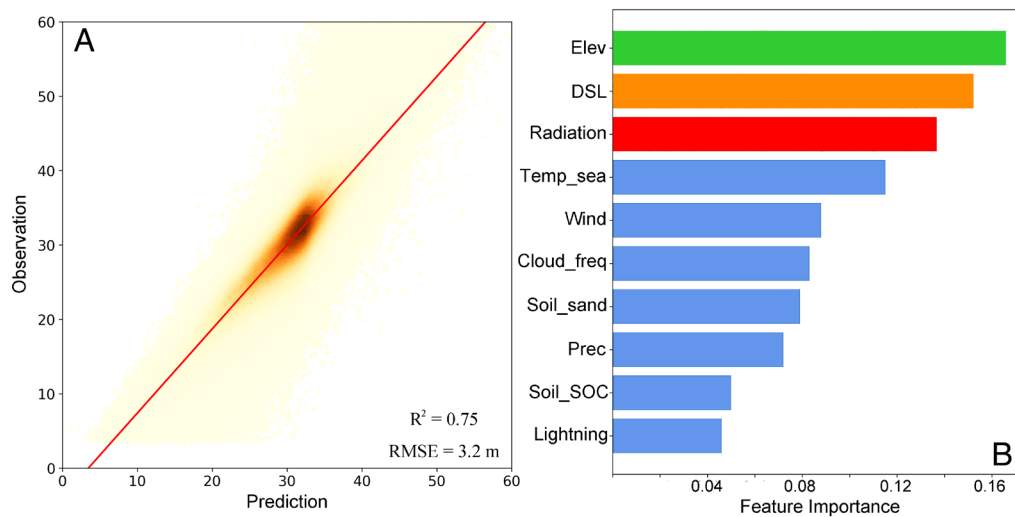


Fig. 2. (A) Comparison between canopy height observations in GEDI L2A and predictions from random forest model. (B) Feature importance values for the explanatory drivers (Table 1) in the random forest model of forest canopy height. In context of this study, Feature importance provides a relative measure of the importance of each explanatory environmental driver in predicting forest canopy height variation. The Feature importance values for a given model sum to unity. Elevation (green bar) has the highest feature; The bar colors correspond to the colors used in Fig. 3 to depict the spatial distribution of the different environmental factors.

drivers in determining canopy height variation. Increases in average wind speed from 1.5 m s^{-1} to 2.5 m s^{-1} are associated with a $\sim 4 \text{ m}$ decline in average canopy height from $\sim 30 \text{ m}$ to $\sim 26 \text{ m}$, but above 2.5 m s^{-1} , the relationship is relatively flat (Fig. 4E). Cloudiness generally has a positive effect on canopy height: Increasing cloudiness from 60 to 80% is associated with an approximately 6 m increase in average canopy height from 26 m to 32 m (Fig. 4F).

Since the marginal analysis above does not account for interactions among environmental drivers on canopy height, we conducted an additional analysis that reveals significant two-way interactions between elevation, DSL, and solar radiation on tropical forest canopy height (SI Appendix, Fig. S2). Regarding the interactions between DSL and elevation, canopy height is negatively related to DSL for elevations above 50 m, but below this value, the relationship becomes relatively flat (SI Appendix, Fig. S2A). Regarding the interactions between solar radiation and DSL, canopy height increases with solar radiation when DSL is shorter than 2 mo; however, when DSL is longer than 4.5 mo, the effect of solar radiation becomes negative (SI Appendix, Fig. S2B). Finally, regarding the interactions between solar radiation and elevation, when incoming solar radiation is above $17,000 \text{ kJ m}^{-2} \text{ d}^{-1}$, canopy height is positively related to elevation. However, below this value, canopy height increases with elevation at intermediate altitudes (around 700 m) but then either plateaus or declines slightly as elevation increases further (SI Appendix, Fig. S2C). Another notable finding is that the combined effects of variation in solar radiation and dry season length (SI Appendix, Fig. S2B) and the combined effects of variation in solar radiation and elevation on canopy height (SI Appendix, Fig. S2C), are associated with canopy height variability of approximately 6 m, which is not captured in the marginal analysis Fig. 4C.

Discussion

The spaceborne GEDI lidar instrument provides full lidar waveform retrievals specifically designed for measuring vegetation structure at global scales (29). Our analysis identifies significant correlations between tropical forest canopy height and a suite of environmental drivers (Fig. 1C), which together explain 75% of

variation in canopy height (Fig. 2A). As seen in Figs. 2B and 3, elevation and DSL are the two most important predictors both regionally and locally.

Previous studies have shown that climatic gradients along with historical events have been found to mediate canopy height at large spatial scales, with water availability playing a pivotal role (24, 26, 27, 38). However, canopy height estimates in these earlier studies were derived from either sparse global field measurements or modeled values produced by combining satellite LiDAR data, rather than direct LiDAR observations and as a consequence, may have underestimated canopy height (25). SI Appendix, Fig. S9 shows that spatial averaged canopy height over the pantropical region from Simard et al. (25) has comparable values with GEDI L2A data, but is lower in Southeast Asia (average difference: -6 m) (Fig. 1C).

Elevation is known to strongly influence a number of environmentally relevant drivers including spatial variation in soil properties, hydrological conditions, and microclimate. Previous studies have documented the influence of elevation on forest canopy heights at local (39–42), regional (18, 21), and continental scales (26). However, the trends in how canopy height changes along elevational gradients varied across the studies: the pattern of increasing canopy height with elevation observed in this study (Fig. 1C) accords with findings from two previous studies (21, 41). However, other studies have found unimodal (40) and monotonically decreasing (39) patterns of canopy height across elevational gradients. One reason for these differing relationships is likely to be the differing elevation ranges examined in these studies. In this analysis, the canopy height dataset excluded measurements from elevations greater than 1,500 m (see Methods Summary section), while other local or regional measurements were conducted in montane elevation transects spanning elevations 200 to 3,100 m (39, 40). Consistent with these studies, although the correlation analysis shows that elevation generally has a positive effect on tropical forest canopy height (Fig. 2C), the marginal analysis reveals that the relationship becomes negative when elevation is greater than 600 m (Fig. 4A). A common explanation for the positive effects of elevation on canopy height in low elevation areas is the reduced frequency of inundation as elevation increases (43). Regarding the negative effects of elevation on

Table 1. Final drivers used to estimate canopy height in the random forest model

Name	Definition	Unit	Source	Resolution
Elev	Ground elevation	m	SRTM	30 m
DSL	Dry season length	month	Princeton	0.25°
Radiation	Incoming solar radiation	W/m ²	WorldClim	1 km
Temp_sea	Temperature seasonality	°C	WorldClim	1 km
Wind	Wind speed	m/s	WorldClim	1 km
Cloud_freq	Cloud frequency	%	EarthEnv	1 km
Sand	Soil sand percentage	%	OpenLand	250 m
Prec	Precipitation	mm/month	WorldClim	1 km
SOC	Soil organic matter	g/kg	OpenLand	250 m
Lightning	Lightning strikes	flashes/month	TRMM	0.25°

canopy height found at higher elevations, a number of mechanisms have been proposed, including periodic wind disturbances (39), constrained leaf expansion by lower temperatures (40), and/or limited solar radiation (42).

The second-most important environmental predictor of forest canopy height was DSL (Fig. 2B), which exhibits a threshold type relationship with minimal effects on canopy height when DSL is less than 4 mo followed by a significant drop in canopy height when DSL exceeds 4 mo (Fig. 4B). This nonmonotonic effect of DSL is likely due in part to the interacting effects of other environmental drivers. In particular, low DSL values tend to be associated with lower solar radiation in areas such as the Western Amazon (*SI Appendix, Fig. S3 B and C*)—both of which tend to increase canopy height. The two other water availability-related drivers included in the analysis, precipitation and soil sand fraction, also exhibited significant univariate relationships with tropical forest canopy height (Fig. 1C); however, their effects were relatively weak after accounting for the influence of other explanatory drivers (Fig. 2B). The influence of DSL found in this study is consistent with findings of Klein et al. (27), who found that precipitation minus potential evapotranspiration (a measure of water availability) was a strong predictor of forest canopy height variation. The primary mechanism by which DSL, precipitation, and sand fraction influence forest canopy height is via soil moisture: Long dry seasons, low precipitation, and high sand fractions all tend to increase water stress, increasing the likelihood of hydraulic failure and tree mortality, particularly for tall trees (44). However, high rainfall events (>3,000 mm y⁻¹), which are often associated with strong winds and nutrient leaching, can result in negative effects on tree growth (21).

SI Appendix, Fig. S2 illustrates the interactions between the three dominant drivers of canopy height variation (elevation, DSL, and radiation). Regarding interactions between the effects of DSL and elevation (*SI Appendix, Fig. S2A*), canopy height decreases with increasing DSL across most elevation bands, however, the negative effects of DSL on canopy height are largely absent in low-elevation areas (<50 m). As discussed above, the negative effects of DSL on canopy height seen across most elevation classes likely reflect reductions in soil moisture as DSL increases (27). One potential explanation for the absence of negative DSL effects at very low elevations (<50 m) may be access to groundwater or greater moisture availability, due to proximity to rivers and floodplains (e.g., Amazon floodplains), which mitigates the declines in soil moisture that would otherwise occur with increasing DSL (45, 46). There are no noticeable interactions between the effects of DSL and radiation (*SI Appendix, Fig. S2B*): Across all DSL values, the canopy height increases with higher radiation, and across all values of incoming radiation, canopy height declines

with longer DSL. Regarding interactions between effects of solar radiation and elevation on canopy height (*SI Appendix, Fig. S2C*), when solar radiation is below 17,000 kJ m⁻² d⁻¹, canopy height follows the characteristic nonmonotonic pattern seen in Fig. 4A, i.e., increasing with elevation up to an altitude of approximately 700 m and then declining slightly as elevation increases further. As discussed earlier, a number of mechanisms have been proposed for this pattern. However, when solar radiation is high (greater than 17,000 kJ m⁻² d⁻¹), canopy height increases monotonically with increasing elevation (up to 1,200 m). As seen in *SI Appendix, Fig. S3C*, these areas of high radiation are predominantly found in Central Africa, the Guiana Shield forests, and parts of Southeast Asia. The reason for this weaker canopy–height–elevation relationship is, at present, unclear. One potential explanation may be that the higher radiation levels alleviate the effects of cooler temperatures on tropical forest productivity that are typically found high elevations. Consistent with this hypothesis, a recent study has shown that African tropical montane forests share some similar structural properties with lowland forests, including an abundance of large trees, and aboveground biomass values comparable to that of African lowland forests (47). Another potential factor is differences in phylogenetic composition in these regions. For example, the study of African above-ground biomass (47) suggested that the presence of conifers (Podocarpaceae), which generally have relatively high light-use efficiencies, may account for the high similarity in the structural properties of lowland and montane forests in Africa documented in their study. Along similar lines, studies of forests in the Guianan Shield have noted dominance by caesalpinoids, a subfamily of legumes, known for their higher nitrogen and light use efficiency, and that similar dominance by closely related genera also occurs in Central Tropical Africa (48). More generally, the two-way interactions seen in *SI Appendix, Fig. S2* indicate that tropical forest canopy height depends on a complex interplay of multiple environmental drivers, with each factor exerting varying levels of influence depending on location and on its interactions with others environmental drivers.

The LIME methodology enabled identification of the importance of different explanatory drivers and how they vary spatially across the pantropical region: Across all three continents, the most dominant feature influencing canopy height was elevation (Fig. 3A and *SI Appendix, Fig. S1*). In the Amazon floodplain, surface flooding pulses act as a disturbance, profoundly affecting trees in the seedling stage and biological productivity (49). In addition, constant soil saturation, combined with lower concentrations of light capture and growth chemicals in leaves, further constrain tree growth in the floodplain (50). Studies in the central Amazonian floodplain reported that the forest structure in a central Amazonian floodplain becomes more diverse and tree height can

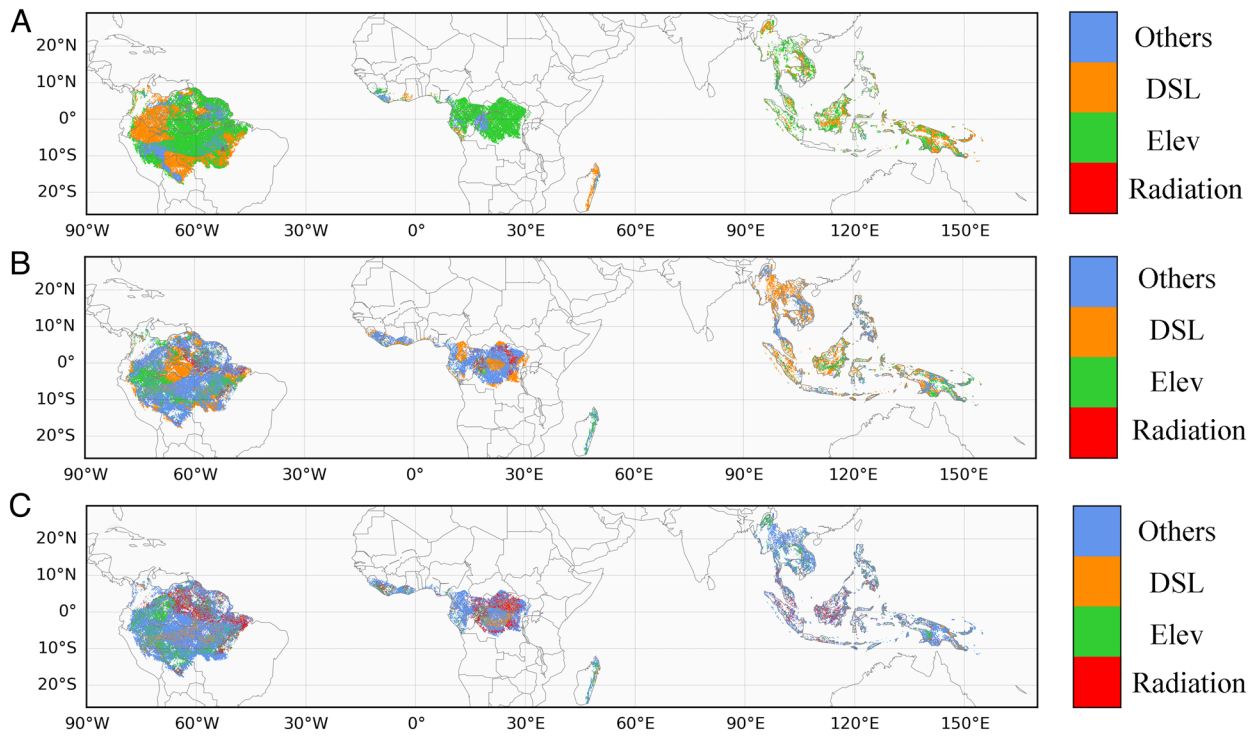


Fig. 3. The spatial variation of the first (A), second (B), and third (C) predictors in controlling local canopy height for Pantropical region derived from the LIME analysis. The remaining environmental predictors (precipitation, temperature seasonality, wind, cloud frequency, sand, soil organic carbon, and wind speed) were grouped into an “Other” category for easier visualization of the three main predictors. A corresponding version of this figure in which the areas labeled as “Other” are colored separately to indicate the relevant specific environmental driver within the “Other” category is shown in [SI Appendix, Fig. S4](#).

increase from 15 m to 45 m with decreasing flooding height, indicating that in low-lying areas, the absence or reduced frequency of flooding at higher elevations has a generally positive impact on canopy height (43). The negative effects of inundation on canopy height are also likely to apply in other low elevation sites in parts of Africa and Southeast Asia. In other areas, such as the Andes (51, 52), Central Africa (53), and Southeast Asia (39), tropical forest canopy height decreases along elevation gradients in higher elevation areas due to a combination of drivers, including periodic disturbances by strong winds, constrained leaf expansion by lower temperature, or limited solar radiation (e.g., west Gabon see [SI Appendix, Fig. S3C](#)).

Dry season length was the second dominant explanatory driver of canopy height over 25% of Amazon and Southeast Asia, but less than 10% of Africa ([SI Appendix, Fig. S1](#)). In the southern Amazon and northern Southeast Asia, forests are exposed to relatively long dry season (DSL > 5 mo, [SI Appendix, Fig. S4C](#)) and many trees may drop a significant portion of their leaves and reduce stomatal conductance to minimize water loss during the dry season. However, in the western Amazon and parts of Borneo where DSL is less than 2 mo, the concurrent low solar radiation and high precipitation may colimit vegetation productivity and growth rates (54).

In summary, we have assessed the spatial variation of forest canopy height in tropical regions using the first spaceborne LiDAR specifically designed to characterize 3D forest structure. Our results show that elevation and dry season length were the most important drivers in determining tropical forest canopy height both regionally and locally. Our findings have several important implications. First, understanding the environmental determinants of spatial variation in canopy height is crucial for improving forest growth and global carbon cycle models. Elevation, dry season length, and solar radiation play important roles in determining canopy height, impacting carbon storage

estimates and therefore allowing more precise carbon accounting in ecosystem and biosphere models (55, 56). Second, the fitted relationship between canopy height and climate drivers can be used to estimate the canopy height potential and consequently, carbon sequestration potential of tropical forests (57). Regions that are optimal for long-term carbon storage can potentially provide low-cost, high-yield carbon mitigation opportunities; however, careful consideration is needed to ensure that these objectives align with conservation and restoration goals (58, 59). Finally, our findings regarding the environmental drivers of forest canopy height also highlight the vulnerability of tropical forest canopy structure to climate change, such as the recent increases in dry season length observed in the southern Amazon (60, 61). These insights regarding the environmental drivers of forest canopy height can inform that effective forest management practices avoid potentially catastrophic tipping points in ecosystem function (62, 63).

One limitation of our analysis concerns the environmental correlates of extremely tall trees. While relatively rare globally, there is considerable interest in the occurrence extremely tall trees because of their disproportionately high biomass and their roles in influencing forest ecosystem processes and diversity (64). Interestingly, the LIME analysis also identifies wind as the most dominant explanatory driver of forest canopy height in the region the northeastern portion of the Brazilian Amazon ([SI Appendix, Fig. S4](#)). This accords with the results of a recent study using airborne lidar data, which found that the environmental drivers influencing the occurrence of extremely tall trees (>70 m) in the Brazilian Amazon were different from the general canopy height variation across the region, with low wind speed in northeastern portion of the Brazilian Amazon being most important predictor of their occurrence (19).

In addition, the identification of primary forest regions may have failed to consider the edge effect on forest structure. Tropical forests

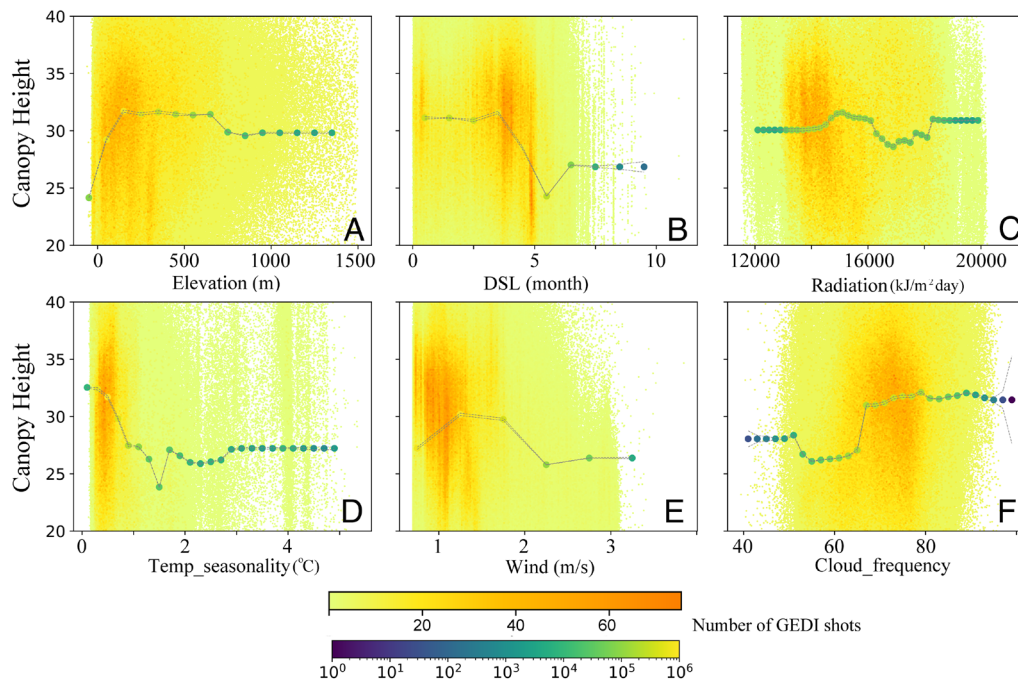


Fig. 4. The marginal plot obtained for the first six important environmental drivers (A: elevation; B: DSL; C: radiation; D: temperature seasonality; E: wind speed and F: cloud frequency) in the random forest model, keeping the other drivers constant at the average values. A corresponding version of this figure showing the relationships plotted in relation to a more complete range of height values within the GEDI dataset is shown in *SI Appendix, Fig. S5*. The upper color legend shows the number of GEDI shots in the scatterplot and the lower color legend shows the number of GEDI shots associated with each dot of the marginal line.

near edges generally show reduced canopy height and density compared to interior forests, as trees are more exposed to environmental stressors and are more susceptible to natural disturbances (65). These conditions often result in higher tree mortality, lower biomass, and accelerated degradation in edge areas (66). Recent work suggests that the extent of forest affected by edges is greater than previously estimated (67), indicating that a significant portion of tropical primary forests may be at increased risk of degradation.

Furthermore, our study excluded tropical forest islands such as Hawaii, tropical dry forests, and secondary forests. Future investigations of the environmental determinants of forest canopy height in these forests are also needed. These analyses will be more challenging however because of the need for knowledge about the nature, magnitude, and timing of human disturbance impacts and fire disturbances that act alongside the effects of underlying environmental conditions in these areas. Finally, one additional challenge in analyzing global-scale variation in tropical forest height is the lack of spatially comprehensive measurements of tropical forest composition. Forest composition influences canopy height through a variety of mechanisms, including species-specific growth patterns, competitive interactions, niche differentiation, and responses to environmental drivers and disturbances (68–70). Integrating GEDI data with information on forest structure derived from forthcoming SAR mission such as NISAR (71) and BIOMASS (72) and information on forest composition from imaging spectrometry measurements (73) has the potential to further enhance our understanding of the underlying drivers of tropical forest canopy height variation.

Methods Summary

This study examines tropical primary forests in the Amazon Basin, Africa, and Southeast Asia to understand how environmental factors influence tree canopy height. After applying rigorous quality filters to GEDI L2A data from 2019 to 2023, a Random Forest

model was used to identify the key drivers of tree height. Feature importance was assessed through permutation tests, while the LIME framework provided insights into local sensitivity. Marginal analysis further explored how individual environmental factors impact canopy height, offering a detailed view of what shapes tropical forest structures.

Data, Materials, and Software Availability. All figures were produced using Python v.3.6 (<https://www.python.org/downloads/release/python-360/>) (74). All code needed to reproduce the main figures are available at <https://zenodo.org/records/14807700> (75). The Global Ecosystem Dynamics Investigation (GEDI) L2A data was accessed through a NASA Earthdata Search (76). Tropical climate data was obtained from WorldClim (<https://www.worldclim.org/>) (77). Elevation from the Shuttle Radar Topography Mission (SRTM) was downloaded from the EarthExplorer (<https://earthexplorer.usgs.gov/>) (78). Soils information was downloaded from the OpenLand platform (<https://opengeohub.org/>) (79). Cloud frequency was obtained from EarthEnv (<https://www.earthenv.org/cloud>) (80). Dry season length was calculated from the Princeton global meteorological forcing dataset (<https://rda.ucar.edu/datasets/d314000/#>) (81). Lightning data was downloaded from the Tropical Rainfall Measuring Mission (TRMM) satellite (https://ghrc.nsstc.nasa.gov/lightning/data/data_lis_trmm.html) (82).

ACKNOWLEDGMENTS. This research was supported by funding from the Harvard University Climate Solutions Fund and NASA grant award #80NSSC21K0197 "Constraining Terrestrial Biosphere Model Predictions of Current and Future Carbon, Energy, and Water Fluxes With Global Ecosystem Dynamics Investigation (GEDI) Waveform Lidar Measurements Of Above-Ground Ecosystem Structure". We thank the GEDI Instrument Team and GEDI Science Team for their support and guidance with the GEDI data and M. C. Hansen for providing the primary forest extent and forest change maps used in our study. The data analyses in this paper were run on the Faculty of Arts & Sciences Research Computing (FASRC) Cannon cluster supported by the Faculty of Arts & Sciences Division of Science Research Computing (RC) Group at Harvard University. We thank the RC Group Support Team for their assistance in conducting the analyses on the FASRC Cannon cluster. We also thank Dubayah Ralph and two anonymous reviewers for their constructive comments on earlier versions of this manuscript.

1. M. A. Lefsky *et al.*, Estimates of forest canopy height and aboveground biomass using ICESat. *Geophys. Res. Lett.* **32**, 1–4 (2005).
2. S. S. Saatchi *et al.*, Benchmark map of forest carbon stocks in tropical regions across three continents. *Proc. Natl. Acad. Sci. U.S.A.* **108**, 9899–9904 (2011).
3. A. C. Bennett *et al.*, Resistance of African tropical forests to an extreme climate anomaly. *Proc. Natl. Acad. Sci. U.S.A.* **118**, e2003169118 (2021).
4. N. G. McDowell, C. D. Allen, Darcy's law predicts widespread forest mortality under climate warming. *Nat. Clim. Chang.* **5**, 669–672 (2015).
5. A. E. L. Stovall, H. Shugart, X. Yang, Tree height explains mortality risk during an intense drought. *Nat. Commun.* **10**, 4385 (2019).
6. U. Roll, E. Geffen, Y. Yom-Tov, Linking vertebrate species richness to tree canopy height on a global scale. *Glob. Ecol. Biogeogr.* **24**, 814–825 (2015).
7. R. Cazzolla Gatti, A. Di Paola, A. Bombelli, S. Noce, R. Valentini, Exploring the relationship between canopy height and terrestrial plant diversity. *Plant Ecol.* **218**, 899–908 (2017).
8. R. A. Houghton, The emissions of carbon from deforestation and degradation in the tropics: Past trends and future potential. *Carbon Manag.* **4**, 539–546 (2013).
9. G. Grassi *et al.*, The key role of forests in meeting climate targets requires science for credible mitigation. *Nat. Clim. Chang.* **7**, 220–226 (2017).
10. A. S. Antonarakis, S. S. Saatchi, R. L. Chazdon, P. R. Moorcroft, Using Lidar and Radar measurements to constrain predictions of forest ecosystem structure and function. *Ecol. Appl.* **21**, 1120–1137 (2011).
11. L. Ma *et al.*, High-resolution forest carbon modelling for climate mitigation planning over the RGGI region, USA. *Environ. Res. Lett.* **16**, 45014 (2021).
12. K. T. Vierling, L. A. Vierling, W. A. Gould, S. Martinuzzi, R. M. Clawges, Lidar: Shedding new light on habitat characterization and modeling. *Front. Ecol. Environ.* **6**, 90–98 (2008).
13. A. B. Davies, F. Oram, M. Ancrenaz, G. P. Asner, Combining behavioural and LiDAR data to reveal relationships between canopy structure and orangutan nest site selection in disturbed forests. *Biol. Conserv.* **232**, 97–107 (2019).
14. D. C. Marvin *et al.*, Amazonian landscapes and the bias in field studies of forest structure and biomass. *Proc. Natl. Acad. Sci. U.S.A.* **111**, E5224–E5232 (2014).
15. W. Turner *et al.*, Remote sensing for biodiversity science and conservation. *Trends Ecol. Evol.* **18**, 306–314 (2003).
16. S. L. Ustin, J. A. Gamon, Remote sensing of plant functional types. *New Phytol.* **186**, 795–816 (2010).
17. R. Dubayah, R. Knox, M. Hofton, J. B. Blair, J. Drake, "Land surface characterization using Lidar remote sensing" in *Spatial Information for Land Use Management*, M. J. Hill, R. J. Aspinall, Eds. (CRC Press, 2000), pp. 53–66.
18. G. P. Asner *et al.*, Landscape-scale changes in forest structure and functional traits along an Andes-to-Amazon elevation gradient. *Biogeosciences* **11**, 843–856 (2014).
19. E. B. Gorgens *et al.*, The giant trees of the Amazon basin. *Front. Ecol. Environ.* **17**, 373–374 (2019).
20. M. N. Dos-Santos, M. M. Keller, D. C. Morton, User Guide: LiDAR Surveys over Selected Forest Research Sites, Brazilian Amazon, 2008–2018. *ORNL DAAC* (2019).
21. E. B. Gorgens *et al.*, Resource availability and disturbance shape maximum tree height across the Amazon. *Glob. Chang. Biol.* **27**, 177–189 (2021).
22. K. J. Niklas, Maximum plant height and the biophysical factors that limit it. *Tree Physiol.* **27**, 433–440 (2007).
23. L. Banin *et al.*, What controls tropical forest architecture? Testing environmental, structural and floristic drivers. *Glob. Ecol. Biogeogr.* **21**, 1179–1190 (2012).
24. A. T. Moles *et al.*, Global patterns in plant height. *J. Ecol.* **97**, 923–932 (2009).
25. M. Simard, N. Pinto, J. B. Fisher, A. Baccini, Mapping forest canopy height globally with spaceborne lidar. *J. Geophys. Res. Biogeosci.* **116**, G04021 (2011).
26. J. Zhang, S. E. Nielsen, L. Mao, S. Chen, J.-C. Svenning, Regional and historical factors supplement current climate in shaping global forest canopy height. *J. Ecol.* **104**, 469–478 (2016).
27. T. Klein, C. Randin, C. Körner, Water availability predicts forest canopy height at the global scale. *Ecol. Lett.* **18**, 1311–1320 (2015).
28. P. M. Montesano *et al.*, The uncertainty of biomass estimates from modeled ICESat-2 returns across a boreal forest gradient. *Remote Sens. Environ.* **158**, 95–109 (2015).
29. R. Dubayah *et al.*, The Global Ecosystem Dynamics Investigation: High-resolution laser ranging of the Earth's forests and topography. *Sci. Remote Sens.* **1**, 100002 (2020).
30. B. E. Schutz, H. J. Zwally, C. A. Shuman, D. Hancock, J. P. DiMarzio, Overview of the ICESat mission. *Geophys. Res. Lett.* **32**, 1–4 (2005).
31. P. Potapov *et al.*, Mapping global forest canopy height through integration of GEDI and Landsat data. *Remote Sens. Environ.* **253**, 112165 (2021).
32. C. A. Silva *et al.*, Fusing simulated GEDI, ICESat-2 and NISAR data for regional aboveground biomass mapping. *Remote Sens. Environ.* **253**, 112234 (2021).
33. N. Lang, W. Jetz, K. Schindler, J. D. Wegner, A high-resolution canopy height model of the Earth. *Nat. Ecol. Evol.* **7**, 1778–1789 (2023).
34. C. Beer *et al.*, Terrestrial gross carbon dioxide uptake: Global distribution and covariation with climate. *Science* **329**, 834–838 (2010).
35. S. Turubanova, P. V. Potapov, A. Tyukavina, M. C. Hansen, Ongoing primary forest loss in Brazil, Democratic Republic of the Congo, and Indonesia. *Environ. Res. Lett.* **13**, 74028 (2018).
36. M. C. Hansen *et al.*, High-resolution global maps of 21st-century forest cover change. *Science* **342**, 850–853 (2013).
37. L. Breiman, Random forests. *Mach. Learn.* **45**, 5–32 (2001).
38. S. Tao, Q. Guo, C. Li, Z. Wang, J. Fang, Global patterns and determinants of forest canopy height. *Ecology* **97**, 3265–3270 (2016).
39. K. Kitayama, S. I. Aiba, Ecosystem structure and productivity of tropical rain forests along altitudinal gradients with contrasting soil phosphorus pools on Mount Kinabalu, Borneo. *J. Ecol.* **90**, 37–51 (2002).
40. S. Ediriweera, B. M. P. Singhakumara, M. S. Ashton, Variation in canopy structure, light and soil nutrition across elevation of a Sri Lankan tropical rain forest. *For. Ecol. Manag.* **256**, 1339–1349 (2008).
41. A. R. Marshall *et al.*, Measuring and modelling above-ground carbon and tree allometry along a tropical elevation gradient. *Biol. Conserv.* **154**, 20–33 (2012).
42. T. Jucker *et al.*, Topography shapes the structure, composition and function of tropical forest landscapes. *Ecol. Lett.* **21**, 989–1000 (2018).
43. F. Wittmann, J. Schöngart, W. J. Junk, "Phytogeography, species diversity, community structure and dynamics of central Amazonian floodplain forests" in *Amazonian Floodplain Forests. Ecological Studies*, W. Junk, M. Piedade, F. Wittmann, J. Schöngart, P. Parolin, Eds. (Springer, Dordrecht, 2010), vol. 210, pp. 61–102, 10.1007/978-90-481-8725-6_4.
44. E. Adrah *et al.*, Analyzing canopy height patterns and environmental landscape drivers in tropical forests using NASA's GEDI spaceborne LiDAR. *Remote Sens.* **14**, 3172 (2022).
45. F. Wittmann, P. Parolin, Aboveground roots in Amazonian floodplain trees. *Biotropica* **37**, 609–619 (2005).
46. N. Armbrüster, E. Müller, P. Parolin, Contrasting responses of two Amazonian floodplain trees to hydrological changes. *Ecotropica* **10**, 73–84 (2004).
47. A. Cuni-Sanchez *et al.*, High aboveground carbon stock of African tropical montane forests. *Nature* **596**, 536–542 (2021).
48. D. S. Hammond, "Guianan forest dynamics: Geomorphographic control and tropical forest change across diverging landscapes" in *Tropical Forests of the Guiana Shield: Ancient Forests in a Modern World* (CABI publishing, Wallingford, UK, 2005), pp. 343–379.
49. S. K. Hamilton, J. Kelldorfer, B. Lehner, M. Tobler, Remote sensing of floodplain geomorphology as a surrogate for biodiversity in a tropical river system (Madre de Dios, Peru). *Geomorphology* **89**, 23–38 (2007).
50. G. P. Asner *et al.*, Landscape biogeochemistry reflected in shifting distributions of chemical traits in the Amazon forest canopy. *Nat. Geosci.* **8**, 567–573 (2015).
51. C. A. J. Girardin *et al.*, Net primary productivity allocation and cycling of carbon along a tropical forest elevational transect in the Peruvian Andes. *Glob. Chang. Biol.* **16**, 3176–3192 (2010).
52. G. Moser *et al.*, Elevation effects on the carbon budget of tropical mountain forests (S Ecuador): The role of the belowground compartment. *Glob. Chang. Biol.* **17**, 2211–2226 (2011).
53. J. Okello, M. Bauters, H. Verbeeck, J. Kasene, P. Boeckx, Aboveground carbon stocks, woody and litter productivity along an elevational gradient in the Rwenzori Mountains, Uganda. *Biotropica* **54**, 906–920 (2022).
54. F. H. Wagner *et al.*, Climate drivers of the Amazon forest greening. *PLoS One* **12**, e0180932 (2017).
55. M. A. Lefsky, W. B. Cohen, G. G. Parker, D. J. Harding, Lidar remote sensing for ecosystem studies. *BioScience* **52**, 19–30 (2002).
56. G. P. Asner *et al.*, High-fidelity national carbon mapping for resource management and REDD+. *Carbon Balance Manag.* **8**, 1–14 (2013).
57. R. L. Chazdon *et al.*, Carbon sequestration potential of second-growth forest regeneration in the Latin American tropics. *Sci. Adv.* **2**, e1501639 (2016).
58. K. D. Holl, P. H. S. Brancalion, Tree planting is not a simple solution. *Science* **368**, 580–581 (2020).
59. B. B. N. Strassburg *et al.*, Global priority areas for ecosystem restoration. *Nature* **586**, 724–729 (2020).
60. N. S. Debortoli *et al.*, Rainfall patterns in the Southern Amazon: A chronological perspective (1971–2010). *Clim. Change* **132**, 251–264 (2015).
61. R. Fu *et al.*, Increased dry-season length over southern Amazonia in recent decades and its implication for future climate projection. *Proc. Natl. Acad. Sci. U.S.A.* **110**, 18110–18115 (2013).
62. S. I. Higgins, S. Scheiter, Atmospheric CO₂ forces abrupt vegetation shifts locally, but not globally. *Nature* **488**, 209–212 (2012).
63. X. Xu *et al.*, Deforestation triggering irreversible transition in Amazon hydrological cycle. *Environ. Res. Lett.* **17**, 34037 (2022).
64. T. R. Feldpausch *et al.*, Height-diameter allometry of tropical forest trees. *Biogeosciences* **8**, 1081–1106 (2011), 10.5194/bg-8-1081-2011.
65. E. N. Broadbent *et al.*, Forest fragmentation and edge effects from deforestation and selective logging in the Brazilian Amazon. *Biol. Conserv.* **141**, 1745–1757 (2008).
66. K. Brinck *et al.*, High resolution analysis of tropical forest fragmentation and its impact on the global carbon cycle. *Nat. Commun.* **8**, 14855 (2017).
67. C. Bourgoin *et al.*, Human degradation of tropical moist forests is greater than previously estimated. *Nature* **631**, 570–576 (2024).
68. G. B. Bonan, S. C. Doney, Climate, ecosystems, and planetary futures: The challenge to predict life in Earth system models. *Science* **359**, eaam8328 (2018).
69. R. A. Chisholm *et al.*, Scale-dependent relationships between tree species richness and ecosystem function in forests. *J. Ecol.* **101**, 1214–1224 (2013).
70. L. F. Mao *et al.*, Maximum canopy height is associated with community phylogenetic structure in boreal forests. *J. Plant Ecol.* **16**, rtac104 (2023).
71. K. Kellogg *et al.*, "NASA-ISRO Synthetic Aperture Radar (NISAR) mission" in 2020 IEEE Aerospace Conference (Big Sky, MT, 2020), pp. 1–21, <https://doi.org/10.1109/AERO47225.2020.9172638>.
72. S. Quegan *et al.*, The European Space Agency BIOMASS mission: Measuring forest above-ground biomass from space. *Remote Sens. Environ.* **227**, 44–60 (2019).
73. E. N. Stavros *et al.*, Designing an observing system to study the Surface Biology and Geology (SBG) of the Earth in the 2020s. *J. Geophys. Res. Biogeosci.* **128**, e2021JG006471 (2023).
74. Python Software Foundation, *Python Language Reference, version 3.6*. <http://www.python.org>. Accessed 1 June 2023.
75. S. Liu, Python scripts for GEDI analysis. Zenodo. <https://doi.org/10.5281/zenodo.14807699>. Deposited 5 February 2025.
76. R. Dubayah *et al.*, GEDI L2A Elevation and Height Metrics Data Global Footprint Level V002. NASA EOSDIS Land Processes Distributed Active Archive Center (2021). https://doi.org/10.5067/GEDI/GEDI02_A_002. Accessed 5 February 2025.
77. S. E. Fick, R. J. Hijmans, WorldClim 2: New 1km spatial resolution climate surfaces for global land areas. *Int. J. Climatol.* **37**, 4302–4315 (2017).
78. U.S. Geological Survey, Shuttle Radar Topography Mission (SRTM) data set. U.S. Geological Survey (2000). <https://earthexplorer.usgs.gov/>. Accessed 24 August 2022.
79. T. Hengl *et al.*, SoilGrids250m: Global gridded soil information based on machine learning. *PLoS ONE* **12**, e0169748, (2017).
80. A. M. Wilson, W. Jetz, Remotely sensed high-resolution global cloud dynamics for predicting ecosystem and biodiversity distributions. *PLoS Biol.* **14**, e1002415, (2016).
81. J. Sheffield, G. Goteti, E. F. Wood, Development of a 50-year high-resolution global dataset of meteorological forcings for land surface modeling. *J. Climate* **19**, 3088–3111 (2006).
82. R. J. Blakeslee, Lightning Imaging Sensor (LIS) on TRMM Science Data. NASA EOSDIS Global Hydrology Resource Center Distributed Active Archive Center (1998). <http://dx.doi.org/10.5067/LIS/LIS/DATA201>. Accessed 26 August 2022.